Localization of Phospho-β-dystroglycan (pY892) to an Intracellular Vesicular Compartment in Cultured Cells and Skeletal Muscle Fibers in Vivo†

Federica Sotgia,‡,§ Gloria Bonuccelli,‡,§ Mark Bedford,|| Andrea Brancaccio,⊥ Ulrike Mayer,# Mark T. Wilson,▽ Roberto Campos-Gonzalez,▽ James W. Brooks,▽ Marius Sudol,○ and Michael P. Lisanti*,‡

Department of Molecular Pharmacology and The Albert Einstein Cancer Center, Albert Einstein College of Medicine, 1300 Morris Park Avenue, Bronx, New York 10461, Servizio Malattie Neuro-Muscolari, Università di Genova, Istituto Gaslini, Largo Gaslini 5, 16147 Genova, Italy, Department of Carcinogenesis, University of Texas, Smithville, Texas 78957, Istituto di Chimica del Riconoscimento Molecolare (CNR) c/o Istituto di Biochimica e Biochimica Clinica, Università Cattolica del Sacro Cuore, Largo Francesco Vito 1, 00168 Roma, Italy, Wellcome Trust Centre for Cell-Matrix Research, School of Biological Sciences, 3.239 Stopford Building, Oxford Road, M13 9PT, Manchester, United Kingdom, BD Biosciences−Pharmingen, 133 Venture Court, Lexington, Kentucky 40511, and Department of Medicine, Mount Sinai School of Medicine, One Gustave Place, New York, New York 10029

Received November 7, 2002; Revised Manuscript Received April 4, 2003

ABSTRACT: β-Dystroglycan is a ubiquitously expressed integral membrane protein that undergoes tyrosine phosphorylation in an adhesion-dependent manner. Tyrosine 892 is now thought to be the principal site for recognition by the c-Src tyrosine kinase; however, little is known about the regulation of this phosphorylation event in vivo. Here, we generated a novel monoclonal antibody probe that recognizes only tyrosine 892 phosphorylated β-dystroglycan (pY892). We show that upon tyrosine phosphorylation, β-dystroglycan undergoes a profound change in its sub-cellular localization (e.g., from the plasma membrane to an internal membrane compartment). One possibility is that the net negative charge at position 892 causes the redistribution of β-dystroglycan to this intracellular vesicular location. In support of this notion, mutation of tyrosine 892 to glutamate (Y892E) is sufficient to drive this intracellular localization, while other point mutants (Y892F and Y892A) remain at the plasma membrane. Interestingly, our colocalization studies with endosomal markers (EEA1, transferrin, and transferrin receptor) suggest that these phospho-β-dystroglycan containing internal vesicles represent a subset of recycling endosomes. At the level of these internal vesicular structures, we find that tyrosine phosphorylated β-dystroglycan is colocalized with c-Src. In addition, we demonstrate that known ligands for α-dystroglycan, namely, agrin and laminin, are able to induce the tyrosine phosphorylation of β-dystroglycan. Finally, we show that tyrosine phosphorylated β-dystroglycan is also detectable in skeletal muscle tissue lysates and is localized to an internal vesicular membrane compartment in skeletal muscle fibers in vivo. The generation of a phospho-specific β-dystroglycan (pY892) mAb probe provides a new powerful tool for dissecting the role of dystroglycan phosphorylation in normal cellular functioning and in the pathogenesis of muscular dystrophies.

Dystrophin is a large, rodlike cytoskeletal protein, which is found at the inner surface of muscle fibers (*1*). The dystrophin gene is mutated in Duchenne Muscular Dystrophy (DMD), as well as in the dystrophin-deficient *mdx* mouse model (*2*, *3*). Dystrophin associates with the cytoskeleton through its interactions with actin and with the sarcolemma through its presence within a large oligomeric complex, termed the dystrophin−glycoprotein complex (DGC) (*4*).

The dystrophin−glycoprotein complex (DGC) contains two smaller complexes, the (i) dystroglycan complex and the (ii) sarcoglycan complex. Originally identified in skeletal muscle, dystroglycan is encoded by a single transcript that is posttranslationally processed into two interacting subunits of ∼156 and ∼43 kDa, respectively, termed α-dystroglycan and β-dystroglycan (*5*).

α-Dystroglycan is a heavily glycosylated extracellular protein that binds to laminin-2, a component of the basal lamina, and to β-dystroglycan. β-Dystroglycan is a transmembrane protein that binds, on the intracellular side, both dystrophin and the dystrophin-related ubiquitous homologue, utrophin (*6*, *7*). As such, dystroglycan is believed to provide a transmembrane link between the extracellular matrix and the cytoskeleton (*8*). Disruption of the dystrophin−glycoprotein complex underlies the molecular pathogenesis of a

† This work was supported by grants from the National Institutes of Health (NIH), the Muscular Dystrophy Association (MDA), the Breast Cancer Alliance (BCA), and the American Heart Association (AHA), as well as a Hirschl/Weil-Caulier Career Scientist Award (all to M.P.L.).

* Corresponding author. Tel: (718) 430-8828. Fax: (718) 430-8830. E-mail: lisanti@aecom.yu.edu.

‡ Albert Einstein College of Medicine.

§ Università di Genova.

|| University of Texas.

⊥ Università Cattolica del Sacro Cuore.

Wellcome Trust Centre for Cell-Matrix Research.

▽ BD Biosciences−Pharmingen.

○ Mount Sinai School of Medicine.

10.1021/bi0271289 CCC: $25.00
Published on Web 05/22/2003

variety of forms of muscular dystrophy. This suggests that this extracellular matrix−cytoskeletal linkage is critical for maintaining the structural integrity of the sarcolemma (*7*, *9*, *10*).

Interestingly, dystroglycan is expressed in a variety of cell types from early development into adulthood, indicating that its function is not restricted to skeletal muscle fibers. The binding partners of dystroglycan may differ in different cell types and in specialized regions of a single cell type. For example, studies have shown that α-dystroglycan can function as an agrin receptor at the level of neuro-muscular junction (*11*, *12*), but can bind laminin-2 throughout the sarcolemma (*8*, *13*). Additional functions for α-dystroglycan arise from the observations that α-dystroglycan may act as the common receptor for viral and bacterial agents, such as the Arena virus and *Mycobacterium leprae* among others (*14*, *15*).

In addition to the crucial structural role of dystroglycan as an extracellular matrix−cytoskeletal linker, it has recently been proposed that dystroglycan may also function as a dynamic signal transducing molecule. Structurally, the proline-rich cytoplasmic tail of β-dystroglycan provides putative sites of interactions for WW domain and SH3 domain containing proteins. Recent reports have demonstrated that the cytoplasmic tail of β-dystroglycan binds proteins involved in signal transduction processes and cytoskeletal organization, such as the SH3 domain containing protein Grb2 (16), and in clustering neurotransmitter receptors, such as rapsyn (*17*). In addition, dystrophin is known to bind β-dystroglycan through 15 residues at the extreme C-terminus of β-dystroglycan (*6*, *18*).

Recent studies have revealed that the interaction of the C-terminal tail of β-dystroglycan with dystrophin occurs primarily through the WW domain of dystrophin (*19*, *20*). A similar modular binding mechanism was shown to explain the interaction of β-dystroglycan with utrophin, a ubiquitous homologue of dystrophin (*21*). The WW domain is a small protein module of ∼38−40 semiconserved amino acids that is widely distributed among various structural, regulatory, and signaling proteins (*22*, *23*). The WW domain is named after two highly conserved tryptophan (W) residues spaced ∼20−22 amino acids apart. WW domains have been implicated in mediating protein−protein interactions by binding to peptide sequences containing proline-rich motifs, such as PPxY (*24*, *25*). The presence of a conserved and potentially phosphorylatable tyrosine (Y) residue within the WW domain binding motif (PPxY) prompted early speculation on its regulatory role in WW domain−ligand binding, possibly serving as a molecular switch between WW and SH2 domains (*26*). However, only recent studies have provided supporting evidence for this proposal (*27*).

Significant progress in understanding the role of β-dystroglycan in signaling came from the observation that β-dystroglycan undergoes c-Src-induced tyrosine phosphorylation at its extreme C-terminus (*27*, *28*). Phosphorylation of β-dystroglycan is strictly dependent on the presence of tyrosine residue 892 within the PPxY motif, which also functions as a ligand for WW domain containing proteins (*27*, *28*). Interestingly, tyrosine phosphorylation of β-dystroglycan at this site blocks its interaction with the WW domains of dystrophin and utrophin (*28*, *29*). Furthermore, tyrosine phosphorylation of β-dystroglycan within the PPxY motif was found to act as a binary regulatory switch to inhibit the binding of WW domain containing proteins, while promoting the recruitment of SH2 domain containing proteins (*27*).

Here, we directly examine the phosphorylation of β-dystroglycan on tyrosine 892 in vivo. For this purpose, we generated and extensively characterized a novel phospho-specific monoclonal antibody probe that selectively recognizes only tyrosine 892 phosphorylated β-dystroglycan (pY892). The generation of a phosphospecific β-dystroglycan (pY892) mAb probe provides a new powerful tool for dissecting the role of dystroglycan phosphorylation in normal cellular functioning and in the pathogenesis of muscular dystrophies.

MATERIALS AND METHODS

Materials. Antibodies and their sources were as follows: anti-β-dystroglycan IgG (mouse mAb, Novocastra), anti-placental alkaline phosphatase IgG (rabbit pAb, Zymed Laboratories Inc.), anti-phospho-tyrosine IgG (rabbit pAb, BD Biosciences−Pharmingen), anti-c-Src IgG (rabbit pAb SRC-2, Santa Cruz Biotech, Inc.), anti-transferrin receptor IgG (rabbit pAb, Cymbus Biotechnology Ltd.), anti-EEA1 (rabbit pAb, Calbiochem), anti-caveolin-1 IgG (rabbit pAb, N-20, Santa Cruz Biotech, Inc.), and anti-caveolin-3 IgG (mouse mAb, clone 26, BD Biosciences−Pharmingen). The cDNA encoding human c-Src WT in the pUSEamp CMV-based vector was purchased from Upstate Biotechnology, Inc. A variety of other reagents were purchased commercially: cell culture reagents were from Gibco-BRL, Agrin (550-AG) was from R&D Systems, Inc.; Laminin (L-2020), Fibronectin (S-5171), and Poly-Lysine (P-1524; MW >300 000) were from Sigma; and transferrin, a tetramethylrhodamine conjugate (T-2872), was from Molecular Probes. Custom synthesis of tyrosine phosphorylated peptides was performed by Genemed Synthesis, Inc. (Irvine, CA).

Construction of cDNAs. The construction of the alkaline phosphatase-tagged β-dystroglycan (AP-βDG) was as previously described (*19*). Briefly, AP-βDG is a fusion protein carrying the transmembrane and cytoplasmic domain of β-dystroglycan fused to the ectodomain of alkaline phosphatase (AP). The constructs encoding AP-βDG (Y892F), AP-βDG (Y892A), and AP-βDG (Y892E) were generated via PCR mutagenesis using oligonucleotides. To obtain the complete sequence for αβ-dystroglycan, RT-PCR was performed using murine skeletal muscle mRNA as the template (*30*). The cDNA segment was linked in frame to the signal peptide sequence of human basement membrane protein BM-40. A cDNA fragment corresponding to the entire coding sequence of αβ-DG and BM40 was inserted into the pCEP Pu/ AC7 plasmid using *XhoI* and *HindIII* cloning sites (*31*). The cDNAs encoding full-length caveolin-1 and caveolin-3 were subcloned into pCB7, a mammalian expression vector driven by the cytomegalovirus (CMV) promoter (*32*−*35*).

Hybridoma Production. A monoclonal antibody to phospho-β-dystroglycan was generated by immunization of Balb/c female mice with a β-dystroglycan peptide phosphorylated on tyrosine 892 (residues 881−895; KNMTPYRSPPP(pY)-VPP). Mice showing the highest titer of immunoreactivity in RSV-transformed cells were used to create fusions with

myeloma cells using standard protocols (*36*). Positive hybridomas were cloned twice by limiting dilution and injected into mice to produce ascites fluid. IgGs were purified by affinity chromatography on protein A-Sepharose.

Cell Culture and Transfection. Cos-7 and 293T cells were grown in DME supplemented with glutamine, antibiotics (penicillin and streptomycin), and 10% fetal calf serum (*33*). Constructs were transiently transfected into Cos-7 cells alone or in combination with c-Src using the Effectene transfection reagent (Qiagen), as per the manufacturer's instructions, and analyzed 36 h post-transfection. Constructs were transiently transfected into 293T cells using using a modified calcium phosphate precipitation method and analyzed 36 h post-transfection.

Immunoblot Analysis. Cells were lysed in boiling sample buffer (*37*). Samples were then collected and boiled for a total of 5 min. Samples were homogenized using a 26 g needle and a 1 mL syringe. To prepare lysates from murine skeletal muscle fibers, muscle tissue was harvested, minced with a scissor, and solubilized with boiling lysis buffer (10 mM Tris, pH 8; 50 mM NaCl; 1% SDS) containing phosphatase inhibitors. Protein lysates were resolved by SDS PAGE (10% acrylamide) under reducing conditions and transferred to nitrocellulose membranes (Schleicher and Schuell). The protein bands were visualized with Ponceau S (Sigma). Membranes were blocked with 4% nonfat dried milk in TBST (20 mM Tris-HCl, 150 mM NaCl, 0.1% Tween 20) supplemented with 1% bovine serum albumin (BSA). For phospho-tyrosine antibodies, membranes were blocked with 4% BSA in TBST. Blots were then incubated at room temperature for 1 h with primary antibody diluted in 1%BSA. Horseradish peroxidase-conjugated secondary antibodies were used to visualize bound primary antibodies with the Supersignal chemiluminescence substrate (Pierce).

Peptide Competition. Cos-7 cells were transiently transfected with AP-βDG and c-Src in combination and subjected to preparative SDS−PAGE. After transfer, the nitrocellulose sheet was cut into strips and incubated with anti-phospho-β-dystroglycan (pY892) IgG alone or in combination with peptides. Horseradish peroxidase-conjugated secondary antibodies (1:6000 dilution, Pierce) were used to visualize bound primary antibodies with the Supersignal chemiluminescence substrate (Pierce).

Immunofluorescence Microscopy. The procedure was performed as we previously described (*38*). Transfected Cos-7 were fixed for 30 min in PBS containing 2% paraformaldehyde. Fixed cells were rinsed with PBS and then incubated in permeabilization buffer (PBS; 0.2% BSA; 0.1% Triton X-100) for 10 min. The cells were then treated with 25 mM NH_4Cl in PBS for 10 min to quench free aldehyde groups, washed with PBS, and successively labeled with a 1:100 dilution of anti-phospho-β-dystroglycan (pY892) IgG (mAb clone 14a). After washing with PBS (3×), cells were incubated with a secondary antibody [fluorescein (FITC)-conjugated goat anti-mouse antibody (Jackson Immunochemicals)]. Cells were then washed with PBS (3×), and slides were mounted with Slow-Fade anti-fade reagent (Molecular Probes). A CCD camera mounted on an Olympus microscope was used for detection of bound secondary antibodies. For double-labeling experiments, the appropriate primary polyclonal antibody (pAb) was incubated along with anti-phospho-β-dystroglycan mAb and detected with lissamine-rhodamine (LRSC)-conjugated goat anti-rabbit antibodies (Jackson Immunochemicals).

Transferrin Internalization Assay. Cos-7 cells were transiently transfected with an alkaline phosphatase-tagged construct containing the cytoplasmic tail of β-dystroglycan (AP-βDG) and c-Src. After 36 h, cells were preincubated with regular media containing 1% BSA for 30 min at 37 °C. Then, the media was replaced with 1 mL of complete media supplemented with rhodamine-conjugated transferrin (10 μg/mL; Molecular Probes). After incubation at 37 °C for 5−60 min, the cells were washed in PBS and fixed in 2% paraformaldehyde for 30 min. Cells transfected with AP-βDG and c-Src were detected by immunostaining with anti-phospho-β-dystroglycan (pY892) IgG (mAb clone 14a) using an FITC-conjugated secondary antibody.

Purification of Lipid Raft/Caveolae Membrane Fractions. Caveolae-enriched membrane fractions were purified essentially as we previously described (*32*). Briefly, transfected 293T cells were scraped in 0.7 mL of MBS (25 mM MES, pH 6.5, 150 mM NaCl) containing 1% Triton X-100 and homogenized with 10 strokes of a tight-fitting Dounce homogenizer. The samples were mixed with an equal volume of 80% sucrose (prepared in MBS lacking Triton X-100), transferred to the bottom of an ultracentrifuge tube, and overlaid with a discontinuous sucrose gradient (1.4 mL of 30% sucrose, 1.8 mL of 5% sucrose, both prepared in MBS, lacking detergent). The samples were then subjected to centrifugation at 44 000 rpm in a SW60 Sorval rotor for 16 h. A light scattering band was observed at the 5/30% sucrose interface. Twelve 0.375 mL fractions were collected, and 10 μg of each fraction was separated by SDS−PAGE and subjected to immunoblot analysis.

Immuno-Staining of Skeletal Muscle Sections. Gastrocnemius muscles were isolated from C57Bl/6 mice (*39*), rapidly frozen in liquid nitrogen cooled isopentane, and stored in liquid nitrogen. Unfixed frozen sections (6 μm thick) of skeletal muscle were treated with 1% BSA, 10% horse serum, and 0.1% Triton X-100 for 1 h at room temperature. Sections were then incubated with a given primary antibody diluted in PBS containing 1% BSA. After three washes with PBS, sections were then incubated with an FITC-conjugated goat anti-mouse secondary antibody. Finally, the sections were washed three times with PBS, and slides were mounted with Slow-Fade anti-fade reagent.

RESULTS

Characterization of a mAb Probe Specific for Tyrosine 892 Phosphorylated β-Dystroglycan. We and others have recently demonstrated that β-dystroglycan undergoes tyrosine phosphorylation at its extreme C-terminus (*27, 28*). Furthermore, we identified the kinase responsible for this phosphorylation event as the c-Src tyrosine kinase (*27*). Using a deletion mutagenesis approach, we have implicated tyrosine residue 892 as the critical site for this event. However, direct in vivo evidence that β-dystroglycan undergoes tyrosine phosphorylation on residue 892 is lacking.

To resolve this issue, we generated a novel phospho-specific mAb probe that recognizes β-dystroglycan only when phosphorylated on tyrosine 892 (see Materials and Methods). Briefly, a tyrosine phosphorylated β-dystroglycan peptide (KNMTPYRSPPP(pY)VPP, residues 881−895) was

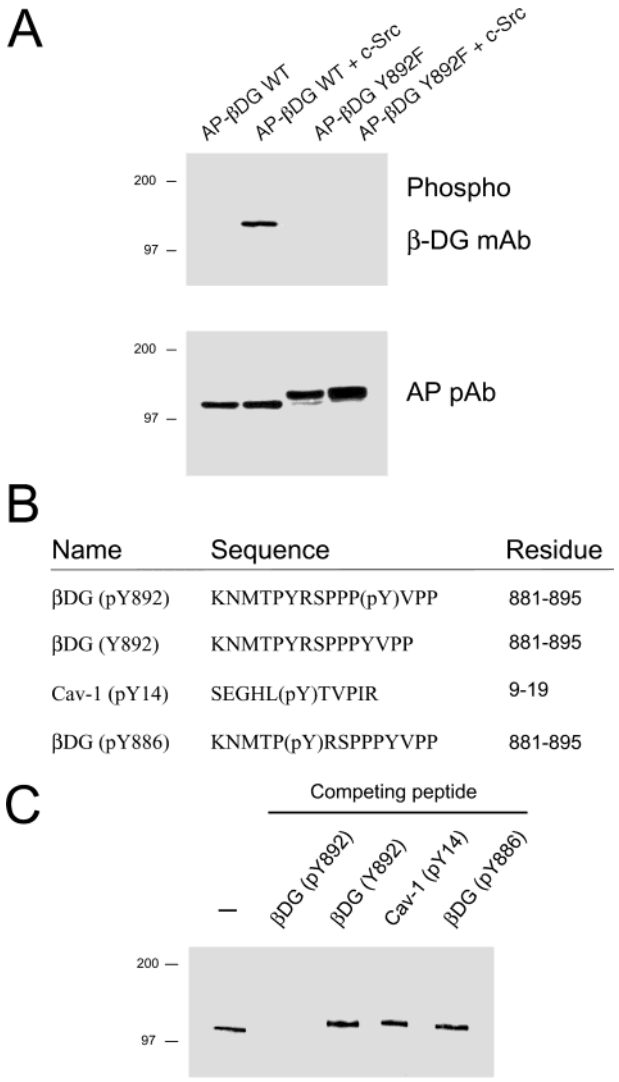

FIGURE 1: Characterization of a mouse mAb probe (cl 14a) that only recognizes β-dystroglycan phosphorylated on tyrosine 892. A β-dystroglycan peptide phosphorylated on tyrosine 892 (KNMTPYRSPPP(pY)VPP, residues 881−895) was used to immunize mice and generate a phospho-β-dystroglycan specific mAb probe. (A) Western blot analysis. Cos-7 cells were transiently transfected with an alkaline phosphatase-tagged form of β-dystroglycan (AP-βDG) and c-Src, alone or in combination. Note that anti-phospho-β-dystroglycan (pY892) IgG only recognizes β-dystroglycan when it is coexpressed with c-Src. Importantly, when tyrosine 892 is mutated to phenylalanine (Y982F), this immuno-reactivity is completely abolished. Immunoblotting with a rabbit pAb that recognizes the alkaline phosphatase epitope tag of the β-dystroglycan construct is shown as a control for equal loading. The mobility of AP-βDG (Y892F) may be upwardly shifted because of a conformational change. (B) β-Dystroglycan phospho-peptides. Sequence of the three β-dystroglycan peptides (pY892, Y892, pY886) and of an irrelevant peptide (Cav-1 pY14) used for the competition assay are shown. (C) Peptide competition. Cos-7 cells were transiently cotransfected with AP-βDG and c-Src and subjected to preparative SDS−PAGE. After transfer to nitrocellulose, the blot was cut into strips and incubated with anti-phospho-β-dystroglycan IgG alone or in combination with peptides. Note that after preincubation with the tyrosine 892 phospho-peptide [the immunogen; βDG (pY892)], anti-phospho-β-dystroglycan (pY892) IgG is no longer able to recognize the phosphorylated protein. In contrast, preincubation with either (i) an unphosphorylated version of the same peptide [βDG (Y892)], (ii) with an irrelevant phospho-peptide peptide [Cav-1 (pY14)], or (iii) with a β-dystroglycan peptide phosphorylated on an adjacent tyrosine [βDG (pY886)] does not affect the immunoreactivity of anti-phospho-β-dystroglycan (pY892) IgG.

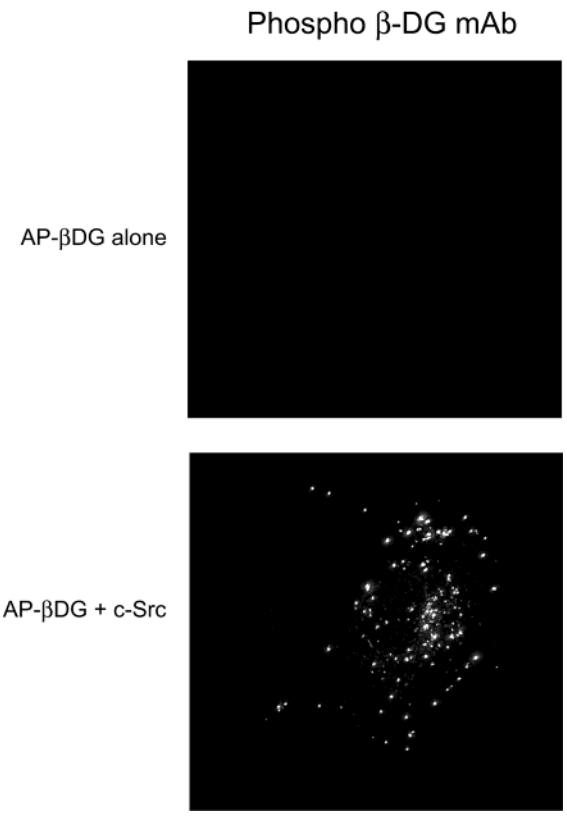

FIGURE 2: Localization of tyrosine 892 phosphorylated β-dystroglycan in Cos-7 cells transiently transfected with c-Src. To examine the localization of tyrosine phosphorylated β-dystroglycan, we transiently transfected Cos-7 cells with an alkaline phosphatase-tagged form of β-dystroglycan (AP-βDG), either alone or in combination with c-Src. Thirty-six h post-transfection, cells were formaldehyde-fixed and immuno-stained with an anti-phospho-β-dystroglycan mouse mAb (cl 14a). As shown in the upper panel, when Cos-7 cells were transfected with AP-βDG alone, little or no immuno-staining with anti-phospho-β-dystroglycan IgG was observed. In cells cotransfected with the cDNA encoding AP-βDG and c-Src, immunostaining with the anti-phospho-β-dystroglycan probe revealed internal membranous/vesicular staining. Most of the cells showed a fluorescent intracellular dotted pattern. A represenative example is shown in the lower panel.

used to immunize mice. Five positive hybridoma clones were obtained (cl 1, 14a, 24a, 27, and 45). Clone 14a gave the strongest immuno-reactivity and was selected for detailed characterization.

Figure 1 demonstrates the specificity of this anti-phospho-β-dystroglycan (pY892) antibody in vivo. Cos-7 cells were transiently transfected with an alkaline phosphatase-tagged construct containing the cytoplasmic tail of β-dystroglycan (AP-βDG) and c-Src, alone or in combination. Note that anti-phospho-β-dystroglycan IgG only recognize tyrosine phosphorylated β-dystroglycan when it is coexpressed with c-Src (Figure 1A). Equal protein loading was assessed using an antibody raised against alkaline phosphatase (AP pAb).

Importantly, when tyrosine 892 is mutated to phenylalanine (Y892F), preventing phosphorylation at this site, this immunoreactivity is completely abolished (Figure 1A). In addition, the mobility of phospho-β-dystroglycan was shifted upward, as we and others have previously noted (*27*, *28*).

We further stringently tested the specificity of anti-phospho-β-dystroglycan (pY892) IgG by peptide competition with β-dystroglycan-derived peptides and with an irrelevant peptide. The sequences of these three β-dystroglycan-based

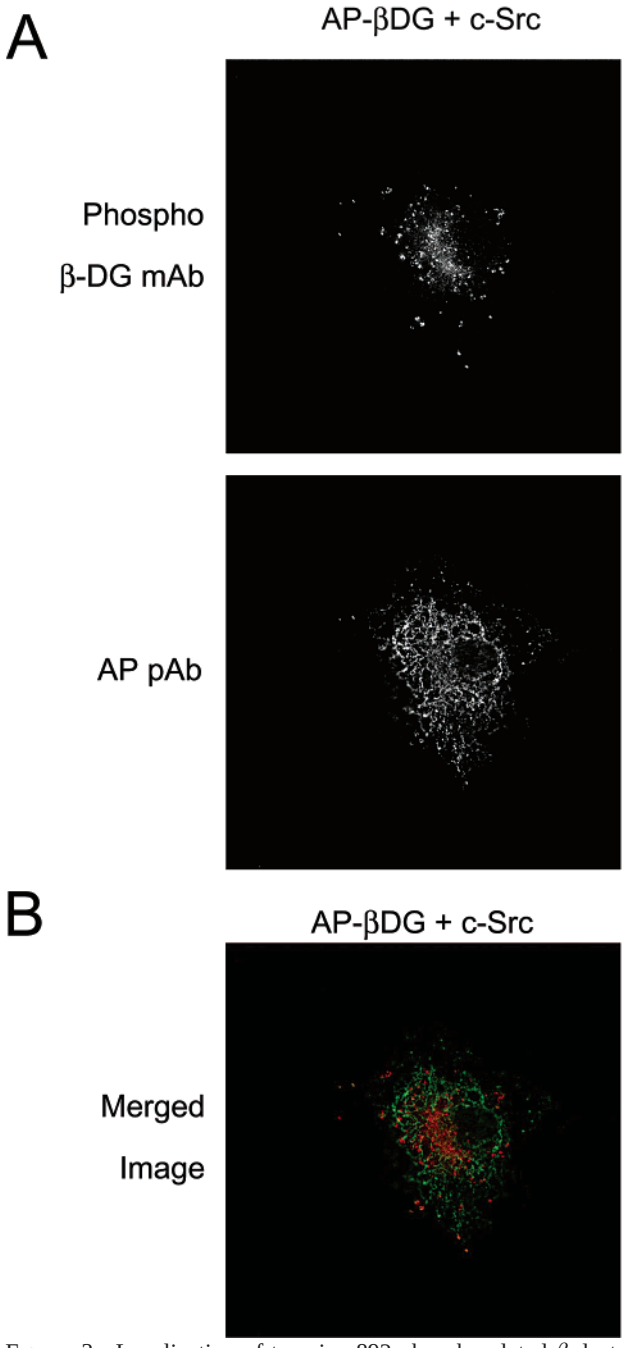

FIGURE 3: Localization of tyrosine 892 phosphorylated β-dystroglycan does not coincide with the pattern observed for total β-dystroglycan. To examine whether the localization of tyrosine phosphorylated β-dystroglycan coincides with total β-dystroglycan, we transiently cotransfected Cos-7 cells with an alkaline phosphatase-tagged form of β-dystroglycan (AP-βDG) and c-Src. (A) Distribution of β-dystroglycan (total vs pY892). Thirty-six h post-transfection, cells were formaldehyde-fixed and doubly immunostained with (i) anti-phospho-β-dystroglycan IgG (mouse mAb cl 14a) and with (ii) an antibody raised against the alkaline phosphatase (AP) tag (rabbit pAb). In cells cotransfected with AP-βDG plus c-Src, immunostaining with anti-phospho-β-dystroglycan appeared as large intracellular dots (upper panel). In contrast, the lower panel shows the membrane-bound distribution of the total β-dystroglycan, as detected by labeling with the AP-tag polyclonal antibody. Note that little or no colocalization is observed. These results indicate that the bulk of β-dystroglycan is not localized in proximity to the major sites of β-dystroglycan tyrosine phosphorylation in vivo. (B) Color overlay. A merged image of the micrographs presented in panel A is shown to better illustrate the relatively nonoverlapping distributions of phospho-β-dystroglycan and total β-dystroglycan within a single cell.

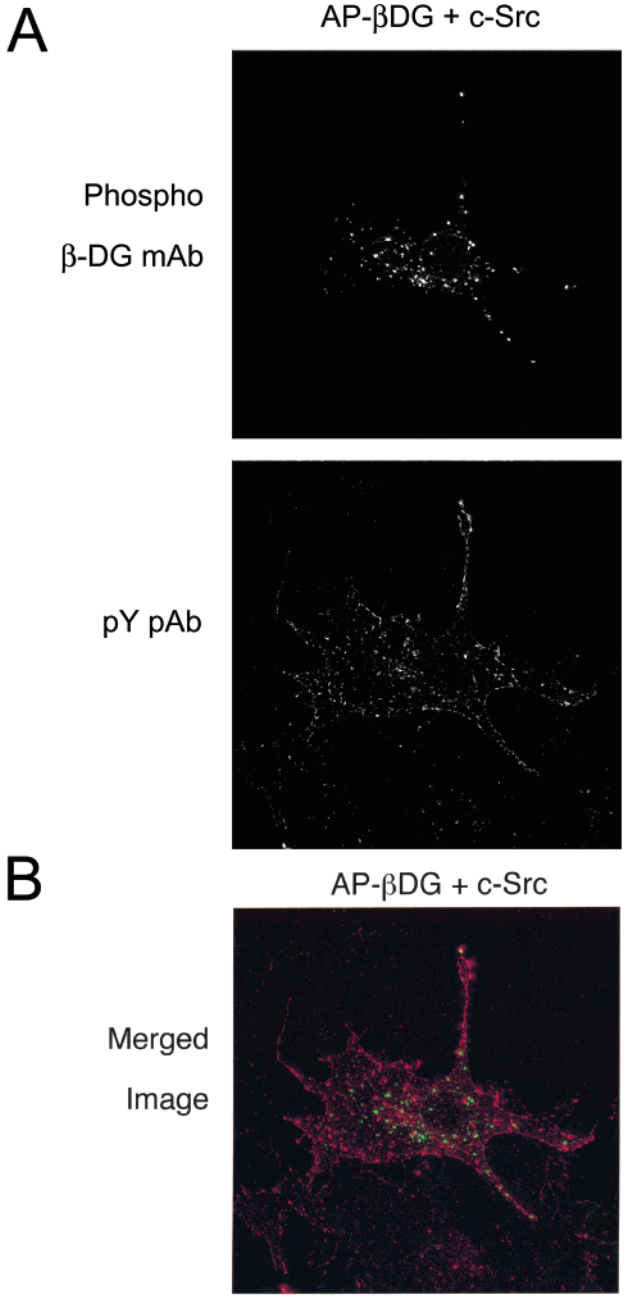

FIGURE 4: Tyrosine 892 phosphorylated β-dystroglycan does not localize to focal adhesions. To examine whether tyrosine phosphorylated β-dystroglycan would localize to focal contacts or adhesions, we transiently transfected Cos-7 cells with an alkaline phosphatase-tagged form of β-dystroglycan (AP-βDG) in combination with c-Src. (A) Phospho-β-dystroglycan vs total phosphotyrosine. Thirty-six h post-transfection, cells were formaldehyde-fixed and doubly immuno-stained with (i) anti-phospho-β-dystroglycan IgG (pY892; mouse mAb cl 14a) and with (ii) an antibody raised against total phospho-tyrosine (pY) (rabbit pAb). Note that tyrosine phosphorylated β-dystroglycan does not colocalize with the major sites of tyrosine phosphorylation. These major sites of tyrosine phosphorylation activity are known to correspond to focal adhesions (40). (B) Color overlay. The merged image clearly indicates that tyrosine phosphorylated β-dystroglycan is not localized in proximity to the major sites of tyrosine phosphorylation in vivo.

peptides (pY892, Y892, pY886) and an irrelevant peptide (Cav-1 pY14) are detailed in Figure 1B. As predicted, immunoreactivity was abolished by preincubation with a 100-fold molar excess of the antigenic peptide (β-DG/pY892) (Figure 1C). Importantly, no inhibitory effect was observed

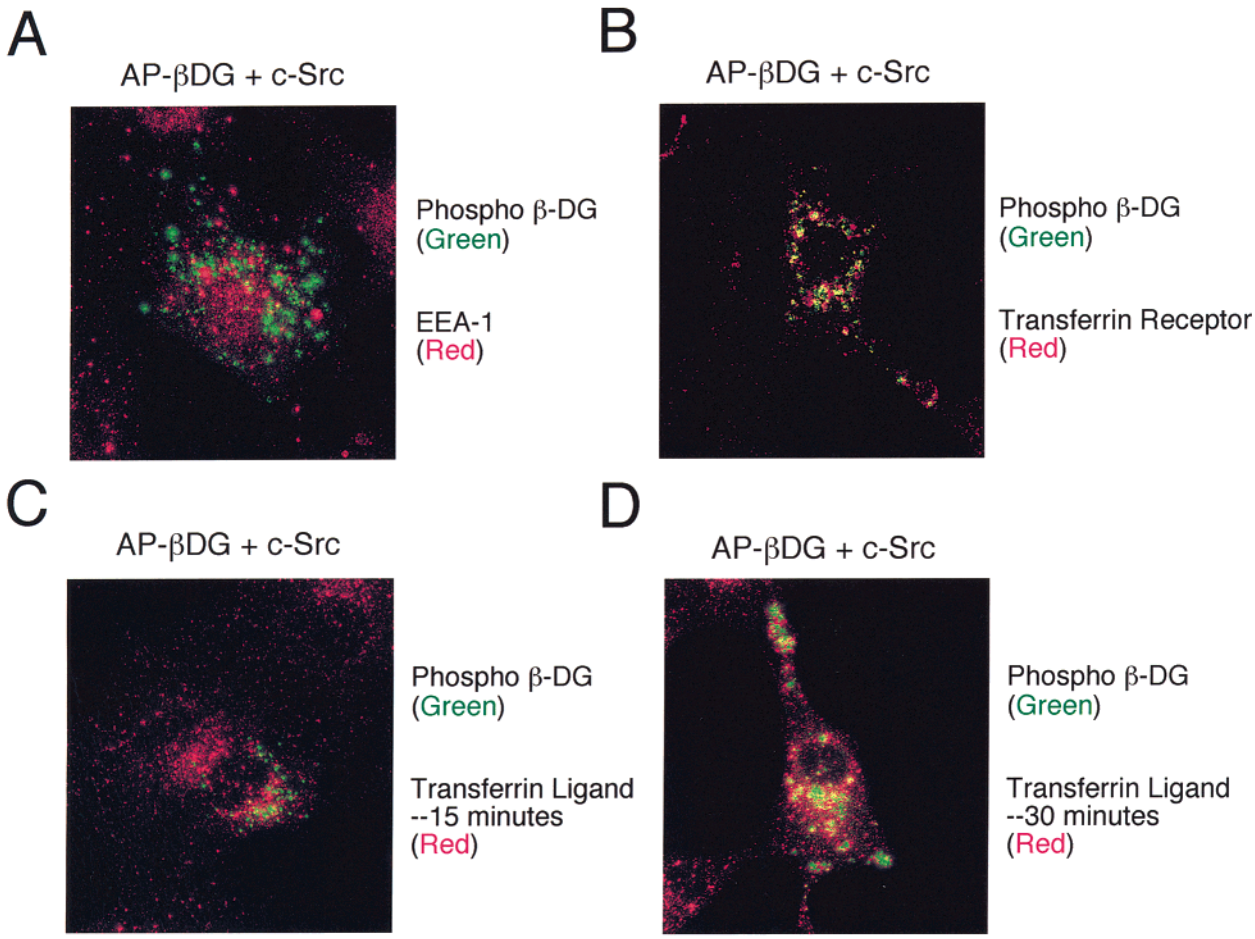

FIGURE 5: Tyrosine 892 phosphorylated β-dystroglycan colocalizes with late endosomes. (A) EEA-1, early endosomal antigen 1. Cos-7 cells were transiently cotransfected with AP-βDG and c-Src. Thirty-six h post-transfection, cells were formaldehyde-fixed and doubly immuno-stained with (i) anti-phospho-β-dystroglycan IgG (mouse mAb, cl 14a; green) and (ii) an antibody raised against EEA 1 (early endosomal antigen 1, rabbit pAb; red). The merged image clearly shows that tyrosine phosphorylated β-dystroglycan does not colocalize with EEA1, a marker for early endosomes. (B) Transferrin receptor. Cos-7 cells were transiently cotransfected with AP-βDG and c-Src. Thirty-six h post-transfection, cells were formaldehyde-fixed and doubly immuno-stained with (i) anti-phospho-β-dystroglycan IgG (mouse mAb, cl 14a; green) and with (ii) an antibody raised against the transferrin receptor (rabbit pAb; red). The merged image clearly indicates that tyrosine phosphorylated β-dystroglycan colocalizes to a large extent with the transferrin receptor (see yellow areas). (C and D) Internalized transferrin ligand. Cos-7 cells were transiently cotransfected with AP-βDG and c-Src. Thirty-six h post-transfection, cells were incubated in normal media supplemented with rodhamine-conjugated transferrin (10 μg/mL; red). After 15 and 30 min at 37 °C, cells were formaldehyde-fixed and immuno-stained with anti-phospho-β-dystroglycan IgG (mouse mAb cl 14a; green). The merged images show that tyrosine phosphorylated β-dystroglycan (green) partially colocalizes with internalized transferrin (red) at a late time point (30 min, panel D) but not at an early point (15 min, panel C). Colocalization appears as yellowish areas.

with the nonphosphorylated version of the same peptide (β-DG/Y892), with an irrelevant phospho-peptide (Cav-1/pY14), or with another β-dystroglycan-based phospho-peptide (β-DG/pY886), in which the phosphorylated tyrosine is located only six amino acids upstream of tyrosine 892. These results directly demonstrate the high selectivity of this novel mAb probe for tyrosine 892 phosphorylated β-dystroglycan.

Phospho-β-dystroglycan (pY892) Is Localized within an Intracellular Membranous Compartment. To assess the localization of phospho-β-dystroglycan (pY892), we next performed immuno-staining on Cos-7 cells transiently transfected with an alkaline phosphatase-tagged construct containing the cytoplasmic tail of β-dystroglycan (AP-βDG) and c-Src, alone or in combination. For this purpose, cells were labeled using the phospho-specific β-dystroglycan antibody (cl 14a). The upper panel of Figure 2 shows that little or no phospho-β-dystroglycan staining is detectable in cells expressing AP-βDG alone. Interestingly, in cells coexpressing AP-βDG and c-Src, we detected a strong signal. Under these conditions, phospho-β-dystroglycan (pY892) was localized to an intracellular membranous compartment, yielding an intriguing dot-like pattern (Figure 2, lower panel).

To evaluate if the localization of phospho-β-dystroglycan (pY892) and total β-dystroglycan coincides, we next performed a series of double-labeling experiments. Cos-7 cells were transiently cotransfected with an alkaline phosphatase-tagged form of β-dystroglycan (AP-βDG) and c-Src.

Immuno-staining with anti-alkaline phosphatase IgG (rabbit pAb) and anti-phospho-β-dystroglycan (pY892) IgG (mouse mAb) revealed that the bulk of total β-dystroglycan was localized to the plasma membrane and was completely segregated from phospho-β-dystroglycan.

Figure 3A shows that phospho-β-dystroglycan (pY892) is localized to a vesicular internal membrane compartment (upper panel). In contrast, total β-dystroglycan shows a characteristic plasma membrane staining pattern (lower panel). Thus, these two labeling patterns appear distinct, suggesting that tyrosine phosphorylated β-dystroglycan is

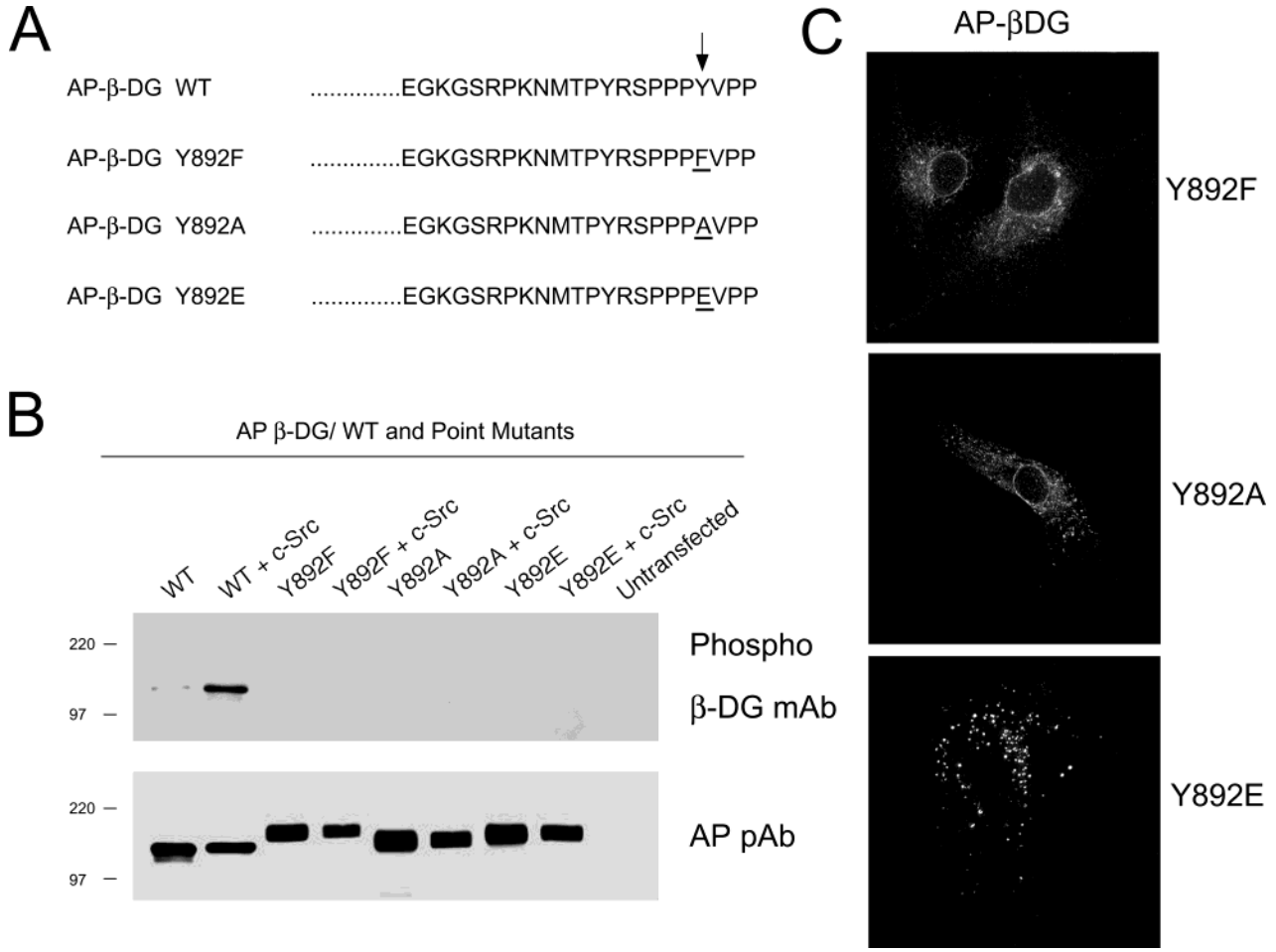

FIGURE 6: Mutation of tyrosine 892 to glutamate (Y892E) redistributes β-dystroglycan to an internal membrane compartment. (A) Constructs. Schematic representation of the four alkaline phosphatase-tagged forms of β-dystroglycan that were utilized: WT (wild-type) and three point mutants Y892F, Y892A, and Y892E. An arrow points at the relevant tyrosine residue (Y892) within the C-terminal PPxY motif. Amino acid substitutions are underlined. (B) Western blot analysis. Cos-7 cells were transiently transfected with mutant versions of AP-βDG, alone or in combination with c-Src. Note that when tyrosine 892 is mutated either to phenylalanine (Y892F), alanine (Y892A), or glutamate (Y982E), anti-phospho-β-dystroglycan (pY892) antibody immuno-reactivity is completely abolished. Immunoblotting with a rabbit pAb that recognizes the alkaline phosphatase tag of the β-dystroglycan construct is shown as a control for equal loading. (C) Immunolocalization of AP-βDG mutants. Cos-7 cells were transiently transfected with each of the cDNAs encoding the above AP-βDG constructs. Thirty-six h post-transfection, cells were formaldehyde-fixed and immuno-stained with a polyclonal antibody directed against the alkaline phosphatase tag (anti-AP IgG; rabbit pAb). Note that the point mutations Y892F and Y892A do not induce any significant changes in the distribution of β-dystroglycan. In striking contrast, the Y892E mutation caused the redistribution of AP-βDG to an intracellular vesicular compartment. Interestingly, this pattern closely resembles the distribution we observed for phospho-β-dystroglycan (pY892). These results are consistent with the notion that a net negative charge at position 892 (either pY or E) causes the redistribution of β-dystroglycan to this intracellular vesicular location.

present in a different region of the cell or that only a subpopulation of β-dystroglycan is tyrosine-phosphorylated. A merged image is also shown to better illustrate that the distribution of total β-dystroglycan and phospho-β-dystroglycan do not coincide (Figure 3B).

As the sites of tyrosine phosphorylation activity are known to correspond to focal adhesions (*40*), we next wondered if phospho-β-dystroglycan (pY892) would colocalize with focal adhesions. Immuno-staining with anti-phospho-tyrosine IgG (rabbit pAb) and anti-phospho-β-dystroglycan (pY892) IgG (mouse mAb) revealed that tyrosine phosphorylated β-dystroglycan does not colocalize with the major sites of tyrosine phosphorylation in Cos-7 cells (Figure 4A). Figure 4B shows a merged image, clearly indicating that tyrosine phosphorylated β-dystroglycan does not localize to focal adhesions.

Phospho-β-dystroglycan (pY892) Shows Colocalization with Endosomal Markers. To identify the nature of the vesicular compartment where phospho-β-dystroglycan (pY892) is localized, we next performed immuno-staining on Cos-7 cells transiently cotransfected with AP-βDG and c-Src. Cells were then double-labeled with the phospho-specific β-dystroglycan monoclonal antibody (cl 14a) and a polyclonal antibody directed against EEA1 (early endosomal antigen 1). Virtually identical experiments were also carried out using a polyclonal antibody directed against the transferrin receptor, which primarily labels both early and recycling endosomes, normally found in the peri-nuclear Golgi region. The resulting merged images are shown in Figure 5, panels A and B. Figure 5A shows that phospho-β-dystroglycan (green) does not colocalize with EEA1, an early endosomal marker (red). However, phospho-β-dystroglycan (green) does colocalize to a large extent with the transferrin receptor (red) (Figure 5B), which is known to be localized mainly to recycling endosomes at steady state.

To further evaluate whether phospho-β-dystroglycan (pY892) localizes to an early or a recycling endosomal

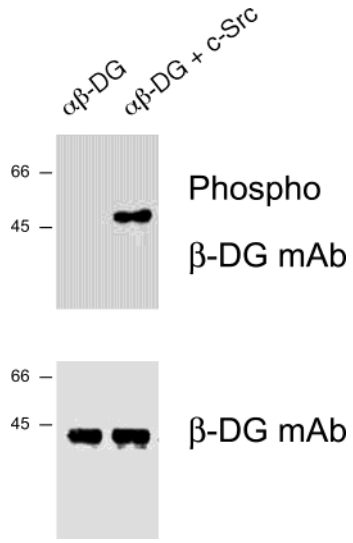

FIGURE 7: Src-induced tyrosine phosphorylation of native αβ-dystroglycan. To rule out any nonspecific effects of the alkaline phosphatase extracellular domain, we next compared the behavior of alkaline-phosphatase tagged β-dystroglycan (AP-βDG) with full-length native αβ-dystroglycan (αβ-DG). For this purpose, we employed a cDNA encoding full-length αβ-dystroglycan. Cos-7 cells were transiently transfected with the full-length cDNA encoding αβ-dystroglycan (αβ-DG) and c-Src, alone or in combination. Note that anti-phospho-β-dystroglycan (pY892) IgG only recognizes β-dystroglycan when it is coexpressed with c-Src. Equal loading was assessed by immunoblot analysis with an antibody that recognizes total β-dystroglycan. Also, note that a characteristic upward mobility shift was observed for tyrosine phosphorylated β-dystroglycan.

compartment, we next performed internalization studies with rhodamine-conjugated transferrin using Cos-7 cells transiently cotransfected with AP-βDG and c-Src. After internalization, the cells were fixed and immuno-stained with anti-phospho-β-dystroglycan IgG (mouse mAb cl 14a). Using this approach, we were able to follow the timing of the internalization of the fluorescent transferrin ligand and evaluate its possible colocalization with phospho-β-dystroglycan. Figure 5C shows that phospho β-dystroglycan (green) does not colocalize with internalized transferring (red) after 15 min of incubation (early endosomes). However, after 30 min of incubation, phospho β-dystroglycan (green) does show colocalization with internalized transferrin (red) (recycling endosomes; Figure 5D). These results are consistent with the observation that phospho β-dystroglycan does not colocalize with EEA1 but does colocalize to a large degree with the transferrin receptor.

Mutation of Tyrosine 892 to Glutamate (Y892E) Redistributes β-Dystroglycan to an Internal Membrane Compartment. Recent findings have suggested that phosphorylation of β-dystroglycan within the C-terminal PPxY motif blocks its interaction with WW domain containing proteins, such as dystrophin and utrophin (*28*, *29*), while favoring the binding with SH2 domain containing proteins (*27*).

Thus, we reasoned that the net negative charge of this phosphorylated tyrosine residue might affect the localization of β-dystroglycan itself. To test this hypothesis, we next generated a panel of AP-βDG mutants, in which the WW-domain ligand (PPxY motif) is modified: Y892F, Y892A, and Y892E. A schematic representation of these mutant constructs is shown in Figure 6A. All three mutations are expected to impede tyrosine phosphorylation of AP-βDG at residue 892. In addition, as glutamate is a negatively charged amino acid, the Y892E mutation is expected to mimic the net negative charge of phosphorylated tyrosine (pY892).

Next, Cos-7 cells were transiently transfected with these AP-βDG mutants, alone or in combination with c-Src. As predicted, all three of these mutants (Y892F, Y892A, and Y892E) are unable to undergo phosphorylation on tyrosine 892 and are, therefore, not recognized by anti-phospho-β-dystroglycan (pY892) IgG (Figure 6B). Equal protein loading was assessed using an antibody raised against alkaline phosphatase (AP pAb).

To visualize the cellular distribution of these AP-βDG mutants, we performed immunofluorescence microscopy on transiently transfected Cos-7 cells. These cells were then labeled with an alkaline phosphatase polyclonal antibody to detect the distribution of total β-dystroglycan.

Figure 6C shows that the point mutations Y892F and Y892A do not induce any significant changes in the distribution of β-dystroglycan. In striking contrast, the Y892E mutation caused the redistribution of AP-βDG to an intracellular vesicular compartment. Interestingly, this pattern closely resembles the distribution we observed for phospho-β-dystroglycan (pY892). These results are consistent with the notion that a net negative charge at position 892 (either pY or E) causes the redistribution of β-dystroglycan to this intracellular vesicular location.

Full-Length αβ-Dystroglycan Behaves in a Similar Fashion as the Alkaline Phosphatase-Tagged Form of β-Dystroglycan. To rule out any nonspecific effects of the alkaline phosphatase extracellular domain, we next compared the behavior of alkaline-phosphatase tagged β-dystroglycan (AP-βDG) with full-length native αβ-dystroglycan (αβ-DG). For this purpose, we employed a cDNA encoding full-length αβ-dystroglycan.

Cos-7 cells were transiently transfected with αβ-DG and c-Src, alone or in combination. In accordance to the previous results, Figure 7 shows that anti-phospho-β-dystroglycan (pY892) IgG recognizes β-dystroglycan only when β-dystroglycan is coexpressed with c-Src. Equal protein loading was assessed using a monoclonal antibody against β-dystroglycan (βDG mAb). It is also interesting to note the characteristic upward mobility shift of tyrosine phosphorylated β-dystroglycan, as compared with total β-dystroglycan—as we and others have previously described (*27*, *28*).

To further corroborate our findings, we next performed immuno-fluorescnce on Cos-7 cells transiently transfected with αβ-DG and c-Src, alone or in combination. When Cos-7 cells were transiently transfected with αβ-DG alone, immuno-staining with anti-phospho-β-dystroglycan (pY892) IgG revealed little or no signal (Figure 8A, upper panel). However, immunostaining with a β-dystroglycan monoclonal antibody revealed a cell surface distribution pattern, as expected (Figure 7A, lower panel).

In contrast, in Cos-7 cells transiently cotransfected with αβ-DG and c-Src, tyrosine phosphorylated β-dystroglycan was localized to an intracellular membrane compartment, while total β-dystroglycan was located at the cell surface (Figure 8B). Thus, these results are consistent with our findings using the alkaline phosphatase-tagged form of β-dystroglycan. Importantly, the overall cellular distribution of AP-βDG and native αβ-DG appeared indistinguishable.

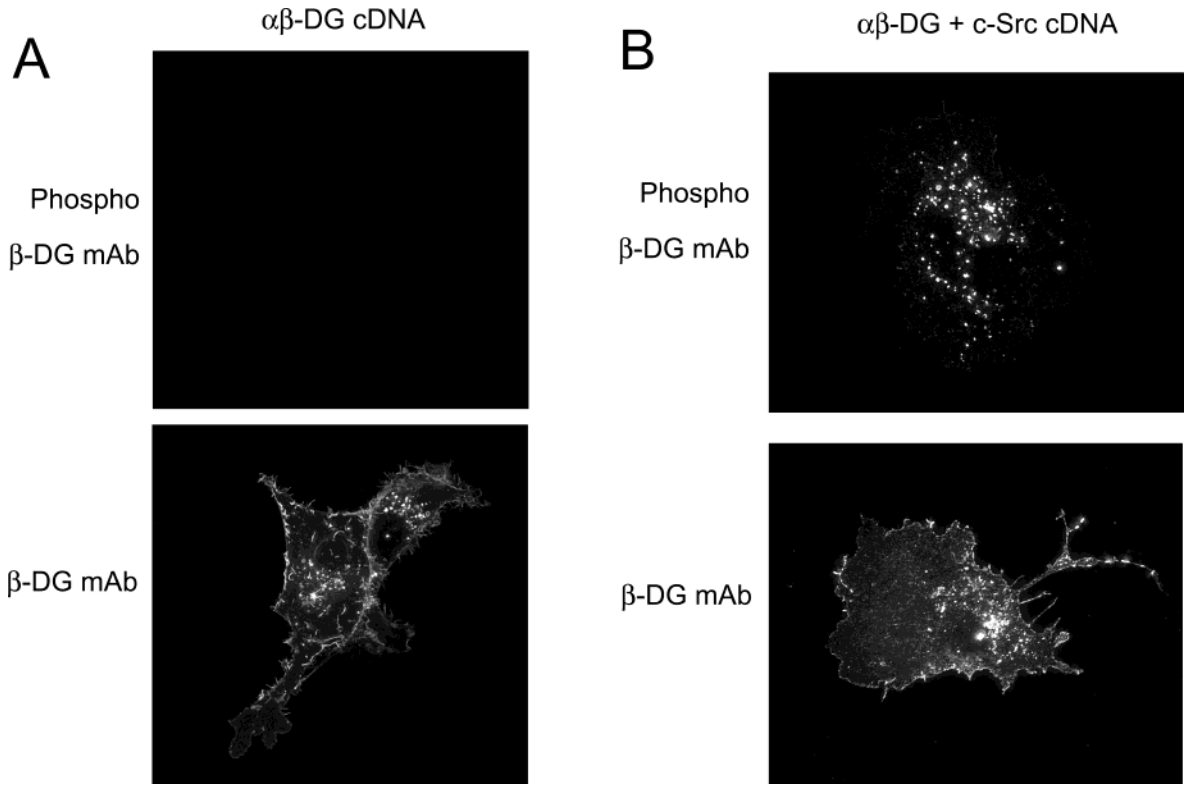

FIGURE 8: Localization of tyrosine phosphorylated native α*β*-dystroglycan. Cos-7 cells were transiently transfected with the full-length cDNA encoding α*β*-dystroglycan (α*β*-DG) and c-Src, alone or in combination. Thirty-six h post-transfection, cells were formaldehyde-fixed and immuno-stained with either (i) anti-phospho-*β*-dystroglycan IgG (pY892; mouse mAb cl 14a) or with (ii) an antibody raised against total *β*-dystroglycan (*β*-DG mouse mAb). Double labeling was not performed, as a polyclonal antibody probe for total *β*-dystroglycan is not commercially available. (A) As shown in the upper panel, when Cos-7 cells were transfected with α*β*-dystroglycan alone, little or no immunostaining with anti-phospho-*β*-dystroglycan IgG was observed. The lower panel shows the cell surface staining of total *β*-dystroglycan in another cell. (B) In cells cotransfected with the full-length cDNA encoding α*β*-dystroglycan and c-Src, immunostaining with the anti-phospho-*β*-dystroglycan probe revealed an intracellular vesicular staining pattern (upper panel). A similar phospho-*β*-dystroglycan staining pattern was also observed using AP-*β*-DG contransfected with c-Src (see Figure 2). The lower panel shows that total *β*-dystroglycan is still targeted to the plasma membrane in c-Src transfected cells, as expected.

Extracellular Matrix Components (Agrin, Laminin, and Fibronectin) Can Function as Ligands During Cell Adhesion to Induce the Phosphorylation of β-Dystroglycan on Tyrosine 892. Recently, α-dystroglycan was shown to function as a receptor for the laminin α2 chain in skeletal muscle, as well as in the central and peripheral nervous system (*5*, *41*). More recently, α-dystroglycan was shown to also act as receptor for agrin, a component of the basal lamina that promotes acetylcholine receptor-induced clustering in skeletal muscle (*42*, *43*). Interestingly, when purified, the agrin receptor was identified as a heteromeric complex of two membrane proteins of 190 and 50 kDa, respectively. Microsequencing of the 190 and 50 kDa subunits revealed great homology with α-dystroglycan and *β*-dystroglycan, respectively (*42*). The shift from the expected 43 kDa to the observed 50 kDa for *β*-dystroglycan was attributed to a carbohydrate modification.

As tyrosine phosphorylated *β*-dystroglycan migrates as a higher molecular mass band of ~50 kDa (see Figure 7), we reasoned that upon binding to α-dystroglycan, agrin might induce the tyrosine phosphorylation of *β*-dystroglycan. To test this hypothesis, Cos-7 cells were transiently transfected with α*β*-dystroglycan (α*β*-DG). After 24 h of serum starvation, the cells were then replated on coverslips coated with poly-lysine, agrin, laminin, or fibronectin.

Interestingly, immuno-staining with anti-phospho-*β*-dystroglycan (pY892) IgG clearly demonstrates that agrin is sufficient to induce the tyrosine phosphorylation of *β*-dystroglycan (Figure 9A, right panel). Similar results were obtained when cells were plated on laminin and fibronectin (Figure 9B). However, as a critical negative control, coating with poly-lysine did not induce any appreciable signal (Figure 9A, left panel). Thus, extracellular matrix components (agrin, laminin, and fibronectin) can function as ligands during cell adhesion to induce the phosphorylation of *β*-dystroglycan on tyrosine 892.

Colocalization of Phospho-β-dystroglycan (pY892) and c-Src in Vivo. Using both in vitro and in vivo approaches, we have previously demonstrated that SH2 domain containing proteins interact with *β*-dystroglycan in a phosphorylation-dependent manner, including c-Src (*27*). As a phospho-*β*-dystroglycan specific probe was not available at that time, we could not determine the cellular location where this event might occur.

To address this issue, we transiently cotransfected Cos-7 cells with α*β*-dystroglycan (α*β*-DG) and c-Src. Next, we performed double-labeling experiments using anti-phospho-*β*-dystroglycan (pY892) IgG (mouse mAb) and antibodies directed against c-Src. Figure 10A shows that tyrosine phosphorylated *β*-dystroglycan precisely colocalizes with c-Src at the level of an intracellular vesicular compartment. A merged color image is shown in Figure 10B, clearly illustrating the overlapping localization of phospho-*β*-dystroglycan and c-Src.

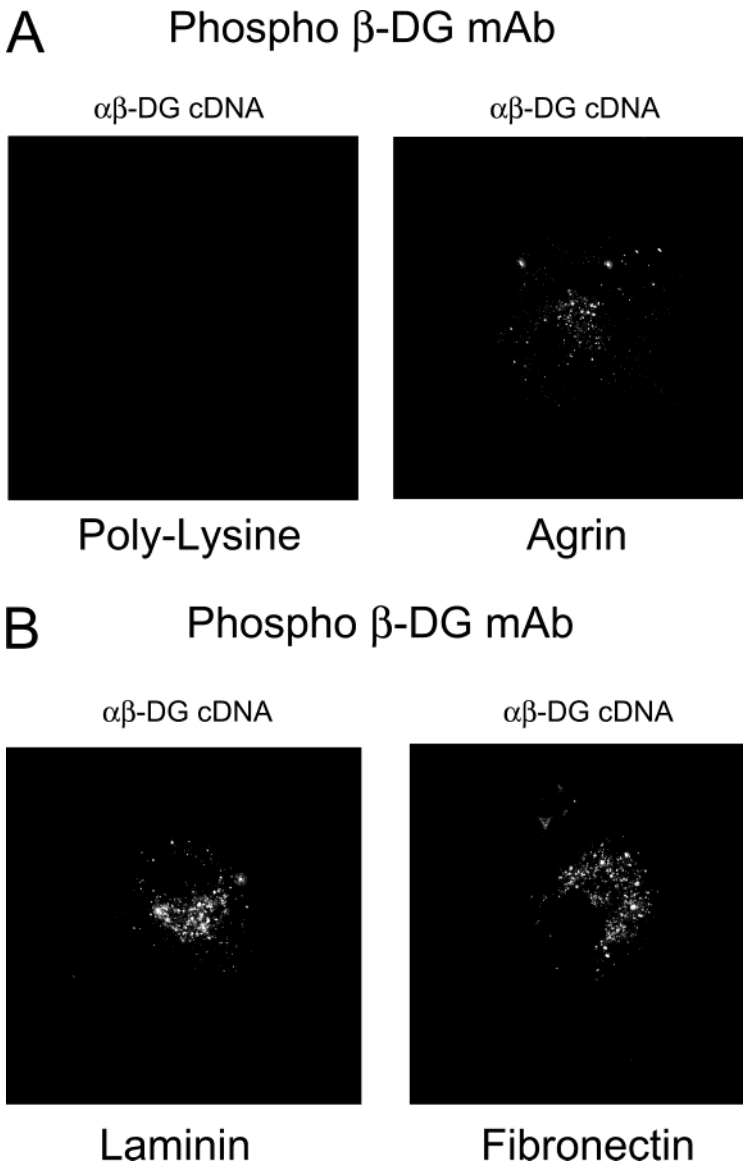

FIGURE 9: Ligand-induced phosphorylation of β-dystroglycan on tyrosine 892. To identify upstream events that induce the tyrosine phosphorylation of β-dystroglycan, Cos-7 cells were transfected with the full-length cDNA encoding αβ-dystroglycan. After 24 h of serum starvation, cells were then trypsinized and replated on either poly-lysine-, agrin-, laminin-, or fibronectin-coated coverslips. After incubation at 37 °C for 20 min after plating, cells were formaldehyde-fixed and immuno-stained with anti-phospho-β-dystroglycan IgG (pY892; mouse mAb cl 14a). Immuno-staining with anti-phospho-β-dystroglycan IgG was detectable only when cells were plated on agrin, laminin, and fibronectin, suggesting that these three ligands are able to induce β-dystroglycan tyrosine phosphorylation (panels A and B). In contrast, when cells were plated on poly-lysine, immunostaing with anti-phospho-β-dystroglycan IgG was extremely faint or absent (panel A).

Phospho-β-dystroglycan Is Targeted to Lipid Raft Domains. As previous studies have shown that β-dystroglycan is normally targeted to lipid rafts/caveolae microdomains (*44*), we next wondered if phospho-β-dystroglycan would still localize to such microdomains. 293T cells were transiently cotransfected with an alkaline phosphatase-tagged construct containing the cytoplasmic tail of β-dystroglycan (AP-βDG) and c-Src. Cell lysates were then subjected to sucrose density gradient ultracentrifugation, a procedure that allows the separation of cholesterol/sphingolipid-enriched domains (aka, lipid rafts) from other membranous and intracellular components (*45*, *46*). Using this method, it is possible to distinguish the caveolae/lipid raft membranes (fractions 5−7) from the total cellular proteins (fractions 8−12). Figure 11 shows that both phospho-β-dystroglycan and total β-dystroglycan are both found in the lipid raft fractions. The difference in the distribution of phospho-β-dystroglycan and total β-dystroglycan (seen by immunofluorescence microscopy) may therefore reflect internalized lipid rafts and cell surface lipid rafts, respectively.

These results are consistent with the notion that the tyrosine phosphorylation of β-dystroglycan may take place in lipid rafts. In support of this possibility, we and others have shown that lipid-modified signaling molecules, such as the c-Src tyrosine kinase, are targeted with high-efficiency to lipid rafts/caveolae membranes (*47*, *48*).

Caveolin Expression Negatively Regulates the Src-Induced Phosphorylation of β-Dystroglycan on Tyrosine 892. Given the association of phospho-β-dystroglycan (pY892) with lipid rafts, we wondered whether caveolins could functionally regulate the tyrosine phosphorylation of β-dystroglycan. In support of this notion, caveolins (Cav-1 and Cav-3) are targeted to lipid raft domains (*32*, *34*, *35*, *49*, *50*), interact with the extreme C-terminal domain of β-dystroglycan, at a

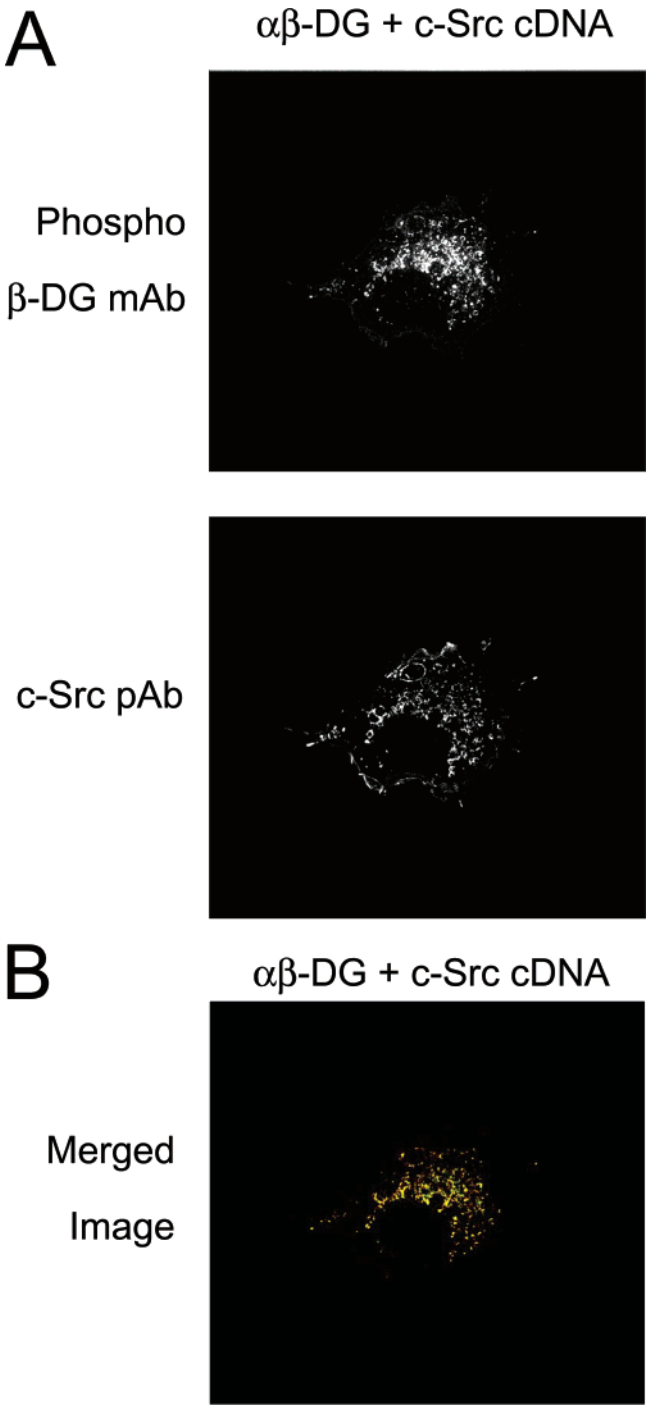

FIGURE 10: Tyrosine phosphorylated β-dystroglycan colocalizes with c-Src in vivo. Cos-7 cells were transiently cotransfected with the full-length cDNA encoding $\alpha\beta$-dystroglycan ($\alpha\beta$-DG) and c-Src. Thirty-six h post-transfection, cells were formaldehyde-fixed and doubly immuno-stained with (i) anti-phospho-β-dystroglycan IgG (mouse mAb) and with (ii) an antibody raised against c-Src (rabbit pAb). (A) Phospho-β-dystroglycan vs c-Src. Note that the distribution of phospho-β-dystroglycan and c-Src precisely coincides. In addition, they both display an intracellular vesicular membrane staining pattern. (B) Color overlay. The merged image clearly indicates that tyrosine phosphorylated β-dystroglycan is colocalized with c-Src in an intracellular vesicular compartment (seen in yellow).

site including tyrosine 892 (*44*), and have been shown to negatively regulate the activity of Src-family tyrosine kinases, including c-Src itself (*38*). On the basis of these findings, we would predict that caveolin expression would inhibit the

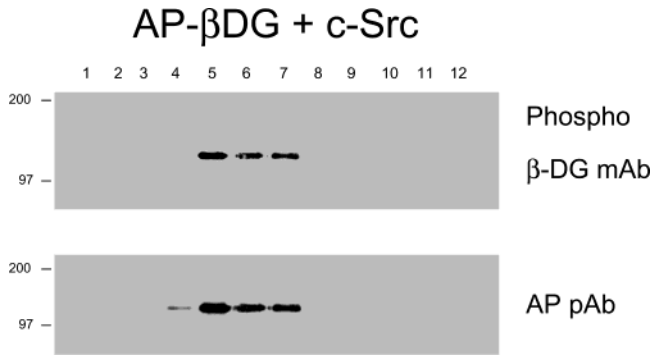

FIGURE 11: Phospho-β-dystroglycan (pY892) is localized to lipid rafts. 293T cells were transiently cotransfected with an alkaline phosphatase-tagged construct containing the cytoplasmic tail of β-dystroglycan (AP-βDG) and c-Src. Cell lysates were subjected to subcellular fractionation after homogenization in a buffer containing Triton X-100. Gradient fractions were collected from the top and analyzed by immunoblotting with (i) anti-phospho-β-dystroglycan IgG (mouse mAb cl 14a) and with (ii) an antibody raised against the alkaline phosphatase (AP) tag (rabbit pAb)—to detect total β-dystroglycan. Note that total β-dystroglycan is found mainly within the lipid rafts (fractions 5−7). Similarly, phospho-β-dystroglycan is clearly targeted to these lipid raft microdomains.

Src-induced phosphorylation of β-dystroglycan on tyrosine 892.

To test this hypothesis, 293T cells were transiently transfected with AP-βDG and c-Src, alone or in combination with Cav-1 and Cav-3. Figure 12 shows that both Cav-1 and Cav-3 dramatically inhibit the Src-induced phosphorylation of β-dystroglycan on tyrosine 892, as predicted. Thus, caveolin expression can serve to functionally modulate the phosphorylation state of β-dystroglycan within caveolae/lipid raft domains.

Localization of Phospho-β-dystroglycan (pY892) in Skeletal Muscle Fibers in Vivo. Is tyrosine-phosphorylated β-dystroglycan detectable in whole tissue samples? Is tyrosine-phosphorylated β-dystroglycan localized to an internal vesicular compartment in vivo? To address these issues, we examined the expression and localization of tyrosine-phosphorylated β-dystroglycan in murine skeletal muscle, a tissue known for its abundant expression of β-dystroglycan.

Skeletal muscle tissue lysates were prepared from C57Bl/6 mice and subjected to Western blot analysis using an anti-phospho-β-dystroglycan (pY892) IgG. In addition, immunoblot analysis with an anti-β-dystroglycan antibody was also performed. Figure 13A shows the upward mobility shift of tyrosine phosphorylated β-dystroglycan, as compared with total β-dystroglycan—as we and others have previously described (*27*, *28*).

Next, frozen sections of murine skeletal muscle tissue were probed with anti-phospho-β-dystroglycan (pY892) IgG. Figure 13B shows that tyrosine-phosphorylated β-dystroglycan is localized within an intracellular vesicular compartment, yielding a dot-like pattern. Importantly, this localization pattern is consistent with what we observed in fibroblastic cells in culture.

As an important internal control, we also immuno-stained skeletal muscle sections with an antibody directed against β-dystroglycan. Figure 13C shows that total β-dystroglycan is confined to the muscle cell plasma membrane (sarcolemma), as expected.

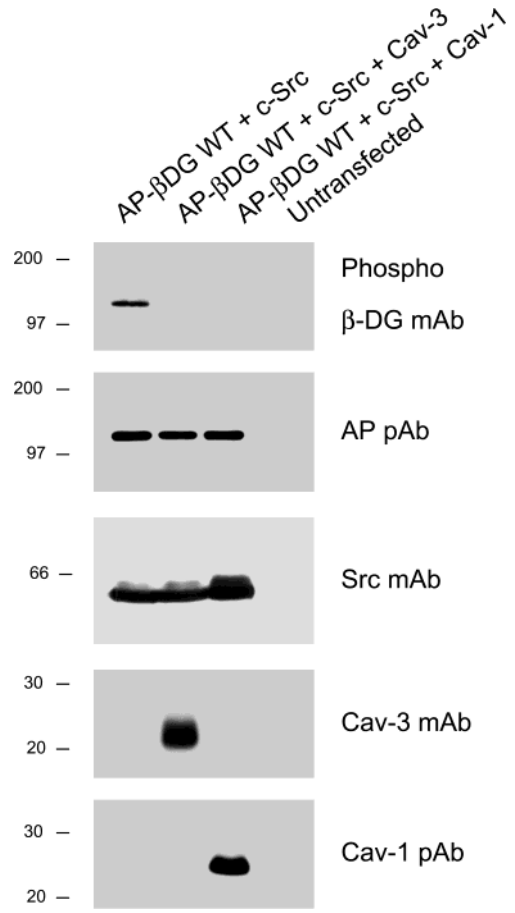

FIGURE 12: Caveolin expression negatively regulates the Src-induced phosphorylation of β-dystroglycan on tyrosine 892. 293T cells were transiently transfected with AP-βDG and c-Src, alone or in combination with Cav-1 and Cav-3. Thirty-six h post-transfection, cell lysates were prepared in hot sample buffer and separated by SDS−PAGE. After transfer to nitrocellulose, samples were subjected to immunoblotting using antibodies directed against phospho-β-DG (pY892), alkaline phosphatase (as an AP-βDG control for equal loading), c-Src, and caveolins (Cav-1and Cav-3). Note that both Cav-1 and Cav-3 dramatically inhibit the Src-induced phosphorylation of β-dystroglycan on tyrosine 892.

DISCUSSION

Dystrophin and dystroglycan are central components of the skeletal muscle dystrophin−glycoprotein complex (DGC), a multimeric complex that spans the cell membrane and links the actin cytoskeleton to the extracellular basement membrane (*8*, *51*). Dystroglycan is thought to provide structural stability to the plasma membrane and to stabilize muscle fibers as they alternately contract and relax (*52*) (i.e., a mechanical role in the transmission of contraction). However, a more recent view attributes a more intricate role to dystroglycan, such that its function is not restricted to the structural integrity of the plasma membrane but includes its participation in signal transduction events.

Initially encoded as a single protein, dystroglycan undergoes posttranslational cleavage to form two interacting subunits, namely, α-dystroglycan and β-dystroglycan. α-Dystroglycan is a peripheral membrane laminin-binding protein, while β-dystroglycan is a transmembrane protein, which anchors dystrophin to the sarcolemmal membrane (*5*, *8*).

Earlier work has shown that dystrophin binds β-dystroglycan through 15 amino acids at the extreme C-terminus of β-dystroglycan (*6*, *18*). An accurate analysis of the binding site between dystrophin and β-dystroglycan revealed that this interaction occurs mainly through the WW domain of dystrophin. Specifically, the WW domain of dystrophin was shown to bind the PPxY motif at the C-terminal tail of β-dystroglycan (*19*, *20*). The clarification of the structure of this binding modality opened unexpected avenues and helped in uncovering new binding partners for β-dystroglycan itself. Caveolin-3, a muscle-specific membrane protein, was found to interact with the C-terminal PPxY motif of β-dystroglycan, at the same or an overlapping site as dystrophin (*44*). Interestingly, this interaction occurs through a WW-like domain in the caveolin-3 protein. As such, caveolin-3 is able to compete with dystrophin for the same binding site on β-dystroglycan and can disrupt the interaction between dystrophin and β-dystroglycan. These results highlight the novel idea that interactions between dystrophin and β-dystroglycan are not static but may be modulated by physiological stimuli.

Recent findings have demonstrated that β-dystroglycan can serve as a substrate of the c-Src tyrosine kinase (*27*). Phosphorylation of β-dystroglycan was found to be strictly dependent on the presence of the tyrosine at residue 892—at the extreme C-terminal of β-dystroglycan (*27*, *28*). This critical residue lies within the PPxY motif, which functions as a ligand for WW domain containing proteins. Interestingly, tyrosine phosphorylation of β-dystroglycan blocks its interaction with the WW domains of dystrophin and utrophin (*28*, *29*). In contrast, the ability of caveolin-3 to bind β-dystroglycan is not affected by the phosphorylation of β-dystroglycan on tyrosine 892 (44). Thus, phosphorylation of β-dystroglycan at this key tyrosine residue within the PPxY motif may determine which molecules can or cannot associate with β-dystroglycan (e.g., acting as a switch to discriminate between available binding partners). Thus, the phosphorylation state of β-dystroglycan may modify the composition, distribution, and possible function of the dystroglycan complex itself. In further support of this notion, tyrosine phosphorylation of the PPxY motif within β-dystroglycan also promotes the recruitment of SH2-domain containing proteins, namely, c-Src, Fyn, Csk, NCK, and SHC (*27*). However, it remains unknown which stimuli can induce the tyrosine phosphorylation of β-dystroglycan.

Here, we directly examined the phosphorylation of β-dystroglycan on tyrosine 892 in vivo. For this purpose, we generated and extensively characterized a novel phospho-specific monoclonal antibody probe that selectively recognizes only tyrosine 892 phosphorylated β-dystroglycan. We find that upon tyrosine phosphorylation, β-dystroglycan undergoes a profound change in its subcellular localization as compared to total β-dystroglycan (e.g., from the plasma membrane to an internal membrane compartment). In addition, as tyrosine phosphorylation occurs primarily at focal adhesions, we next explored the possibility that phosphorylated β-dystroglycan would localize to these sites. However, tyrosine phosphorylated β-dystroglycan shows a localization pattern that overtly diverges from immuno-staining with anti-phospho-tyrosine IgG, suggesting that tyrosine phosphorylated β-dystroglycan does not localize to focal adhesions.

In an attempt to uncover the physiological stimuli that induce the tyrosine phosphorylation of β-dystroglycan, we have shown that known ligands of α-dystroglycan, namely,

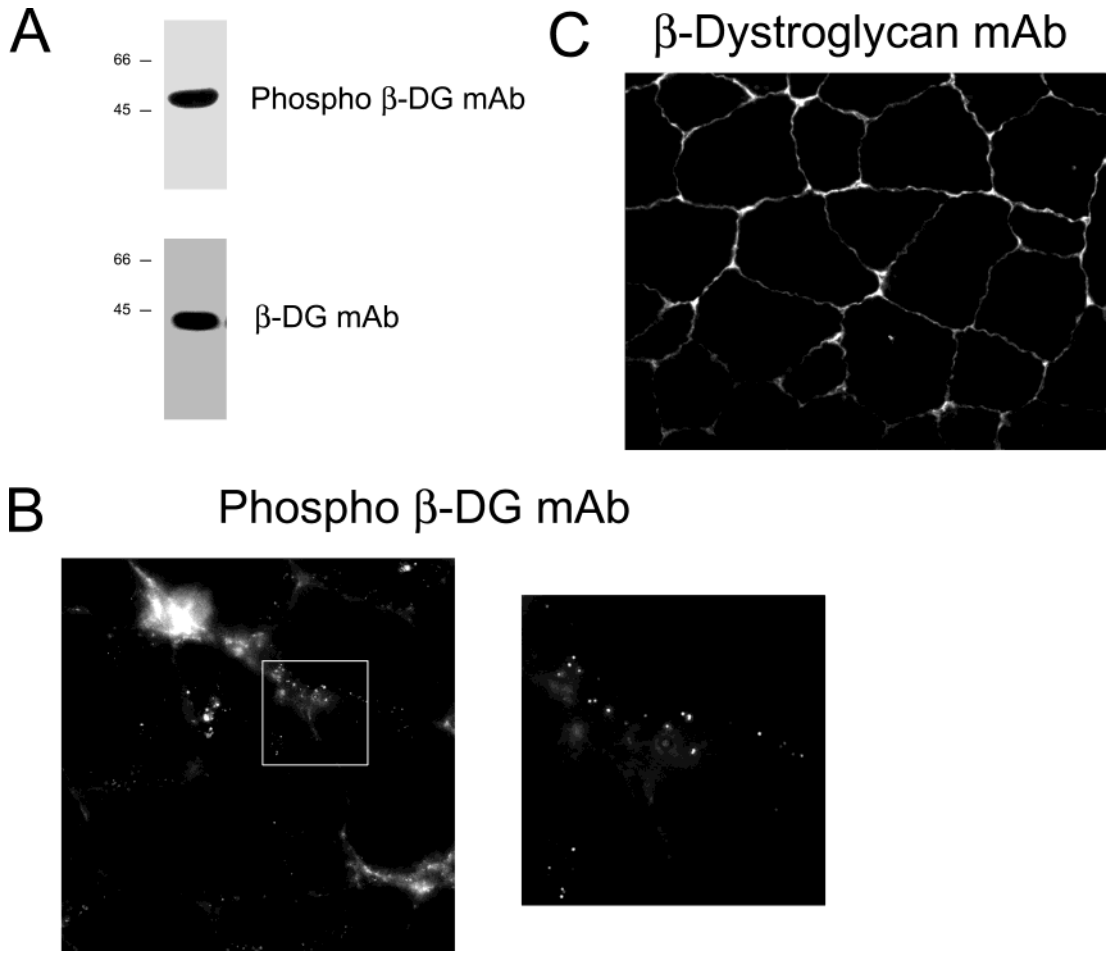

FIGURE 13: Localization of phospho-β-dystroglycan (pY892) in skeletal muscle fibers in vivo. (A) Western blot analysis. Skeletal muscle tissue lysates were prepared from C57Bl/6 mice and subjected to Western blot analysis using anti-phospho-β-dystroglycan (pY892) IgG. In addition, immunoblot analysis with an anti-β-dystroglycan antibody was also performed. Note the characteristic upward mobility shift of tyrosine phosphorylated β-dystroglycan, as compared with total β-dystroglycan—as we and others have previously described (27,28). (B and C) Immunohistochemistry. Frozen sections of skeletal muscle tissue were prepared from C57Bl/6 mice and were probed with anti-phospho-β-dystroglycan (pY892) IgG. Note that tyrosine-phosphorylated β-dystroglycan is localized within an intracellular vesicular compartment that is proximal to the plasma membrane, yielding a dot-like pattern (panel B, see higher magnification inset). As an important internal control, we also immuno-stained skeletal muscle sections with an antibody directed against total β-dystroglycan. In contrast, total β-dystroglycan is confined to the muscle cell plasma membrane (sarcolemma), as expected (panel C).

agrin and laminin, are able to induce the tyrosine phosphorylation of β-dystroglycan. These results strongly support the idea that dystroglycan acts as a signal-tranducing receptor, thereby mediating signaling between the outside and the inside of the cell. Consistent with this idea, tyrosine phosphorylated β-dystroglycan colocalizes with c-Src at the level of intracellular vesicles.

As previous studies have shown that a percentage of β-dystroglycan is normally targeted to lipid rafts/caveolae microdomains (*44*), we next wondered if phospho-β-dystroglycan would still localize to such microdomains. In direct support of this notion, we observed using a biochemical fractionation technique that both phospho-β-dystroglycan and total β-dystroglycan are colocalized within the lipid raft/caveolae fractions. Thus, these results are consistent with the notion that the tyrosine phosphorylation of β-dystroglycan takes place in lipid rafts. In support of this possibility, we and others have shown that lipid-modified signaling molecules, such as the c-Src tyrosine kinase, are targeted with high-efficiency to lipid rafts/caveolae membranes (*47*, *48*).

Given the association of phospho-β-dystroglycan (pY892) with lipid rafts, we wondered whether caveolins could functionally regulate the tyrosine phosphorylation of β-dystroglycan. In support of this notion, caveolins (Cav-1 and Cav-3) are targeted to lipid raft domains (*32*, *34*, *35*, *49*, *50*), interact with the extreme C-terminal domain of β-dystroglycan, at a site including tyrosine 892 (*44*), and have been shown to negatively regulate the activity of Src-family tyrosine kinases, including c-Src itself (*38*). On the basis of these findings, we would predict that caveolin expression would inhibit the Src-induced phosphorylation of β-dystroglycan on tyrosine 892. Here, we show that both Cav-1 and Cav-3 dramatically inhibit the Src-induced phosphorylation of β-dystroglycan on tyrosine 892, as predicted. Thus, caveolin expression can serve to functionally modulate the phosphorylation state of β-dystroglycan within caveolae/lipid raft domains. As such, the internal membranous vesicles containing phosphorylated β-dystroglycan may be internalized lipid rafts/caveolae-like vesicles.

In further support of this notion, we show here that phosphorylated β-dystroglycan colocalizes with endosomal markers (transferrin receptor and its ligand; Figure 5), suggesting that these internalized lipid rafts are indeed endosomes. Similarly, we show that phosphorylated β-dys-

troglycan is localized to an internal membrane compartment in skeletal muscle fibers, while total β-dystroglycan remains at the cell surface. Thus, the difference in the distribution of phospho-bDG and bDG seen by immunofluorescence may simply reflect two dynamic populations of lipid rafts (internalized vs cell surface). Evidence has been presented by other groups that lipid rafts can exist both at the level of the plasma membrane, as well as within internal membrane compartments—such as endosomes (*53*, *54*).

REFERENCES

1. Koenig, M., Monaco, A. P., and Kunkel, L. M. (1988) *Cell 53*, 219−26.
2. Hoffman, E. P., Brown, R. H., and Kunkel, L. M. (1987) *Cell 51*, 919−28.
3. Bulfield, G., Siller, W. G., Wight, P. A., and Moore, K. J. (1984) *Proc. Natl. Acad. Sci. U.S.A. 81*(4), 1189−92.
4. Ervasti, J. M., and Campbell, K. P. (1991) *Cell 66*, 1121−31.
5. Ibraghimov-Beskrovnaya, O., Ervasti, J. M., Leveille, C. J., Slaughter, C. A., Sernett, S. W., and Campbell, K. P. (1992) *Nature 355*, 696−702.
6. Jung, D., Yang, B., Meyer, J., Chamberlain, J. S., and Campbell, K. P. (1996) *J. Biol. Chem. 270*, 27305−10.
7. Winder, S. J. (2001) *Trends Biochem. Sci. 26*, 118−24.
8. Ervasti, J. M., and Campbell, K. P. (1993) *J. Cell Biol. 122*, 809−23.
9. Ervasti, J. M., Ohlendieck, K., Kahl, S. D., Gaver, M. G., and Campbell, K. P. (1990) *Nature 345*(6273), 315−9.
10. Campbell, K. P. (1995) *Cell 80*, 675−9.
11. Fallon, J. R., and Hall, Z. W. (1994) *Trends Neurosci. 17*(11), 469−73.
12. Gee, S. H., Montanaro, F., Lindenbaum, M. H., and Carbonetto, S. (1994) *Cell 77*, 675−86.
13. Ekblom, P., and Timpl, R. (1996) *Curr. Opin. Cell Biol. 8*, 599−601.
14. Rambukkana, A., Yamada, H., Zanazzi, G., Mathus, T., Salzer, J. L., Yurchenco, P. D., Campbell, K. P., and Fischetti, V. A. (1998) *Science 282*(5396), 2076−9.
15. Cao, W., Henry, M. D., Borrow, P., Yamada, H., Elder, J. H., Ravkov, E. V., Nichol, S. T., Compans, R. W., Campbell, K. P., and Oldstone, M. B. (1998) *Science 282*(5396), 2079−81.
16. Yang, B., Jung, D., Motto, D., Meyer, J., Koretzky, G., and Campbell, K. P. (1995) *J. Biol. Chem. 270*, 11711−4.
17. Cartaud, A., Coutant, S., Petrucci, T. C., and Cartaud, J. (1998) *J. Biol. Chem. 273*(18), 11321−6.
18. Rosa, G., Ceccarini, M., Cavaldesi, M., Zini, M., and Petrucci, T. C. (1996) *Biochem. Biophys. Res. Commun. 233*, 272−7.
19. Rentschler, S., Linn, H., Deininger, K., Bedford, M. T., Espanel, X., and Sudol, M. (1999) *Biol. Chem. 380*, 431−42.
20. Huang, X., Poy, F., Zhang, R., Joachimiak, A., Sudol, M., and Eck, M. J. (2000) *Nat. Struct. Biol. 7*(8), 634−8.
21. Tommasi di Vignano, A., Di Zenzo, G., Sudol, M., Cesareni, G., and Dente, L. (200) *FEBS Lett. 14*(471), 229−34.
22. Bork, P., and Sudol, M. (1994) *Trends Biochem. Sci. 19*, 531−3.
23. Sudol, M., Chen, H. I., Bougeret, C., Einbond, A., and Bork, P. (1995) *FEBS Lett. 369*, 67−71.
24. Chen, H. I., and Sudol, M. (1995) *Proc. Natl. Acad. Sci. U.S.A. 92*, 7819−23.
25. Sudol, M., and Hunter, T. (2000) *Cell 103*, 1001−4.
26. Sudol, M. (1996) *Trends Biochem. Sci. 21*, 161−3.
27. Sotgia, F., Lee, H., Bedford, M. T., Petrucci, T., Sudol, M., and Lisanti, M. P. (2001) *Biochemistry 40*(48), 14585−92.
28. James, M., Nuttall, A., Ilsley, J. L., Ottersbach, K., Tinsley, J. M., Sudol, M., and Winder, S. J. (2000) *J. Cell Sci. 113*, 1717−26.
29. Ilsley, J. L., Sudol, M., and Winder, S. J. (2001) *Cell Signal 13*(9), 625−32.
30. Brancaccio, A., Ruegg, M. A., and Engel, J. (1995) *Matrix Biol. 14*, 681−5.
31. Mayer, U., Nischt, R., Pöschl, E., Mann, K., Fukuda, K., Gerl, M., Yamada, Y., and Timpl, R. (1993) *EMBO J. 12*, 1879−85.
32. Sargiacomo, M., Sudol, M., Tang, Z.-L., and Lisanti, M. P. (1993) *J. Cell Biol. 122*, 789−807.
33. Scherer, P. E., Tang, Z.-L., Chun, M. C., Sargiacomo, M., Lodish, H. F., and Lisanti, M. P. (1995) *J. Biol. Chem. 270*, 16395−401.
34. Song, K. S., Scherer, P. E., Tang, Z.-L., Okamoto, T., Li, S., Chafel, M., Chu, C., Kohtz, D. S., and Lisanti, M. P. (1996) *J. Biol. Chem. 271*, 15160−5.
35. Tang, Z.-L., Scherer, P. E., Okamoto, T., Song, K., Chu, C., Kohtz, D. S., Nishimoto, I., Lodish, H. F., and Lisanti, M. P. (1996) *J. Biol. Chem. 271*, 2255−61.
36. Harlow, E., and Lane, D., Eds. (1988) *Antibodies: A laboratory manual*, Cold Spring Harbor Laboratory, Woodbury, NY.
37. Galbiati, F., Volonte′, D., Engelman, J. A., Watanabe, G., Burk, R., Pestell, R. G., and Lisanti, M. P. (1998) *EMBO J. 17*, 6633−48.
38. Li, S., Couet, J., and Lisanti, M. P. (1996) *J. Biol. Chem. 271*, 29182−90.
39. Galbiati, F., Engelman, J. A., Volonte, D., Zhang, X. L., Minetti, C., Li, M., Hou, H. J., Kneitz, B., Edelmann, W., and Lisanti, M. P. (2001) *J. Biol. Chem. 276*(24), 21425−33.
40. Helfman, D. M., E. T., L., Berthier, C., Shtutman, M., Riveline, D., Grosheva, I., Lachish-Zalait, A., Elbaum, M., and Bershadsky, A. D. (1999) *Mol. Biol. Cell 10*(10), 3097−112.
41. Yamada, H., Denzer, A. J., Hori, H., Tanaka, T., Anderson, L. V., Fujita, S., Fukuta-Ohi, H., Shimizu, T., Ruegg, M. A., and Matsumura, K. (1996) *J. Biol. Chem. 271*(38), 23418−23.
42. Bowe, M. A., Deyst, K. A., Leszyk, J. D., and Fallon, J. R. (1994) *Neuron 12*(5), 1173−80
43. Ruegg, M. A., and Bixby, J. L. (1998) *Trends Neurosci. 21*(1), 22−7.
44. Sotgia, F., Lee, J. K., Das, K., Bedford, M., Petrucci, T. C., Macioce, P., Sargiacomo, M., Bricarelli, F. D., Minetti, C., Sudol, M., and Lisanti, M. P. (2000) *J. Biol. Chem. 275*(48), 38048−58.
45. Lisanti, M. P., Tang, Z.-T., Scherer, P., and Sargiacomo, M. (1995) *Methods Enzymol. 250*, 655−68.
46. Song, K. S., Tang, Z.-L., Li, S., and Lisanti, M. P. (1997) *J. Biol. Chem. 272*, 4398−403.
47. Song, K. S., Sargiacomo, M., Galbiati, F., Parenti, M., and Lisanti, M. P. (1997) *Cell. Mol. Biol. 43*, 293−303.
48. Galbiati, F., Volonte, D., Meani, D., Milligan, G., Lublin, D. M., Lisanti, M. P., and Parenti, M. (1999) *J. Biol. Chem. 274*, 5843−50.
49. Lisanti, M. P., Scherer, P. E., Vidugiriene, J., Tang, Z.-L., Hermanoski-Vosatka, A., Tu, Y.-H., Cook, R. F., and Sargiacomo, M. (1994) *J. Cell Biol. 126*, 111−26.
50. Lisanti, M. P., Scherer, P., Tang, Z.-L., and Sargiacomo, M. (1994) *Trends Cell Biol. 4*, 231−5.
51. Yoshida, M., and Ozawa, E. (1990) *J. Biochem. (Tokyo) 108*(5), 748−52.
52. Henry, M. D., and Campbell, K. P. (1996) *Curr. Opin. Cell Biol. 8*(5), 625−31.
53. Gagescu, R., Demaurex, N., Parton, R. G., Hunziker, W., Huber, L. A., and Gruenberg, J. (2000) *Mol. Biol. Cell 11*, 2775−91.
54. Simons, K., and Gruenberg, J. (2000) *Trends Cell Biol. 10*, 459−62.

BI0271289